TRANSIENT STATE IN STANDING WAVE ACCELERATING STRUCTURES

JACEK SEKUTOWICZ

Deutsches Elektronen–Synchrotron DESY, Notkestraße 85, 22607 Hamburg, FRG

Superconducting accelerating cavities can be operated in the pulse mode to lower capital and operating costs of the cryogenic plant. Some additional cost reduction is also possible when the accelerating process takes place already during the fill time, i.e. before the accelerating structures reach the final steady state. Such an operation needs more analysis of the transient state in multicell cavities. In this paper one possible approach to the complete analysis of the transient state in standing wave accelerating structures is presented. The different approach, giving envelope of the transient state, the reader can find in.[1] In this paper set of equations derived from a lumped element replacement circuit model used for the analysis, is solved in a semi-analytic way. The method of solution is based on the classical Laplace transformation aided by some additional numerical calculations. The computed cavity response to the harmonic driving source agrees well with measurements for various types of cavities. As an example, comparison of the transient state measurements and calculations for a 9–cell, 1GHz copper cavity are discussed in more detail. Next, diagrams relating cavity parameters to the time delay at the beginning of the fill and to the phase deviation for the steady state, computed with a program written especially for this analysis are given. Finally, some preliminary computations for structure of the future superconducting linear collider TESLA are discussed.

KEY WORDS: Radio-frequeny, accelerating structures, superconducting cavities

1. INTRODUCTION

The behaviour of standing wave accelerating structures made up of N coupled cells may be analyzed by considering the properties of N coupled Lumped Element Circuits (LEC). Many problems such as correction of machining errors, field pattern sensitivity to cell frequency perturbation, transient states and power deposition by the accelerated beam to parasitic modes, may be investigated by means of the LEC model analysis.[2,3,4] An analogy between an accelerating structure and LEC can be established when the eigenfrequencies of coupled cells, the losses and the cell–to–cell coupling are known. Following, for example, the procedure presented in,[3] one can find these parameters directly from measurements of field patterns, frequencies and Q_s of all passband modes. Standing wave monoperiodic accelerating structures terminated with full end cells (Fig. 1) are usually designed for operation in π–mode. The impedance seen by an accelerated beam has the highest value for this mode
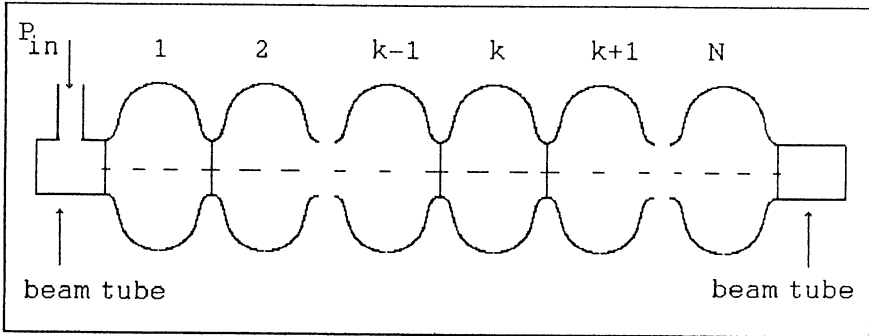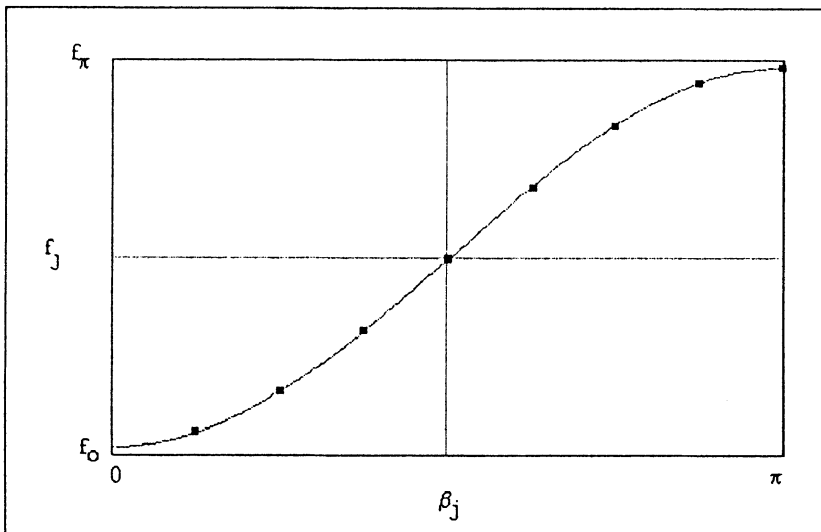
FIGURE 1:   Standing wave monoperiodic structure

compared to the other modes of the fundamental passband, thus an advantageous re-
lation between RF wall losses and the power transferred to the beam can be achieved.

π–mode oscillation, characterized by equal field amplitudes in all cells, and π phase
shift between the neighbouring cells, is achievable in a monoperiodic lossless structure
with full end cells, if their eigenfrequencies are corrected to compensate for periodicity
perturbation caused by the beam tube. Fig. 2 shows fundamental passband dispersion
curves $f_j(\beta_j)$ of two monoperiodic capacitively coupled cavities: with $N = \infty$ and a

FIGURE 2:   Dispersion curves of standing wave monoperiodic structures: $N = \infty$ (solid line), $N = 8$ (dots)

real cavity with finite N and corrected end cells. For the lossless case $\beta_j = \pi \cdot \frac{j}{N}$ determines the pattern of the steady state amplitude, X_{kj}, for each cell k and each resonant frequency f_j, according to the expression:

$$X_{kj} = B \cdot \sin(\beta_j \cdot (k - 0.5)) \qquad (1)$$

B is a factor proportional to the power of the driving source and $j = 1...N$. Dispersion curves are well approximated by formula:

$$f_j = \frac{f_0}{\sqrt{1 + \kappa \cdot \cos(\beta_j)}} \qquad (2)$$

where f_0 is the eigenfrequency of a decoupled cell and κ is the first order coupling between two neighbouring cells. Field pattern and frequency measurements on four well–tuned models of 4–cell 500MHz, 9–cell 1GHz, 9–cell 1.3GHz and 5–cell 1.5GHz showed good agreement with (1) and (2).

Usually, in analogy to signal propagation in waveguides, one describes propagation in the accelerating standing wave structures by the group velocity Vg which is proportional to $| \frac{df}{d\beta} |$. For the structure made of very few cells such an approach seems to be artificial. It can be seen from the dispersion diagram that for $\beta_j \rightarrow \pi$, the group velocity Vg $\rightarrow 0$. The largest value Vg is reached for $\beta_j \rightarrow \frac{\pi}{2}$. Such a different signal propagation along the structure for the π–mode and any mode in the middle of the dispersion curve should cause a visible difference in time delay during the filling. The results presented in,[5] for a 9–cell 1GHz structure showed that this is not the case. The time delay at the beginning of the filling between the signals in the first cell with the driving antenna and the last cell was the same for the π–mode and the $\frac{5\pi}{9}$–mode, which lies in the vicinity of the $\frac{\pi}{2}$–mode.

2. MODEL

In order to investigate these results we use the LEC model as shown in Fig. 3. The electrical properties of the chain of N coupled resonant circuits are matched to the electrical properties of the fundamental mode (TM010) passband of a N–cell cavity with a cell form developed for superconducting (sc) storage ring cavities. The method we use here holds also for any other cell shape if only the first order coupling, either magnetic or electric, is relevant. The fundamental mode of sc storage ring structures has a dominating electric field in the coupling iris, so only the capacitive component of the coupling has been taken into account. The elements L_k, C_k, R_k of each circuit k and coupling capacitors $C_{k,k+1}$ may vary for different k, thus further analysis will not be limited to monoperiodic and well–tuned cavities which here will be only a special case. The mesh currents $x_k(t)$ and the coupling currents $x_{k-1,k}(t)$ must fulfil 2N–1 voltage mesh equations:
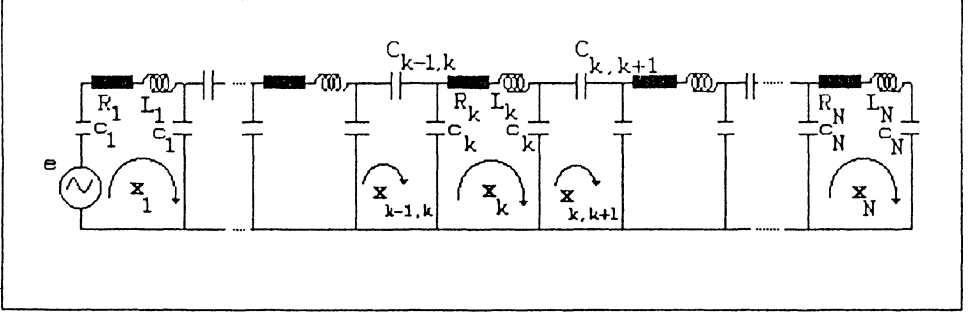
FIGURE 3: LEC used as replacement of the standing wave cavity

$$R_1 \cdot x_1(t) + L_1 \cdot \dot{x}_1(t) + \frac{1}{C_1} \cdot \int_0^t x_1(\tau)d\tau - \frac{1}{C_1} \cdot \int_0^t x_{1,2}(\tau)d\tau = U_{-1}(t)e(t)$$

$$\vdots$$

$$\frac{-1}{C_{k-1}} \cdot \int_0^t x_{k-1}(\tau)d\tau + \left(\frac{1}{C_{k-1}} + \frac{1}{C_{k-1,k}} + \frac{1}{C_k}\right) \cdot \int_0^t x_{k-1,k}(\tau)d\tau$$

$$-\frac{1}{C_k} \cdot \int_0^t x_k(\tau)d\tau = 0$$

$$\frac{-1}{C_k} \cdot \int_0^t x_{k-1,k}(\tau)d\tau + R_k \cdot x_k(t) + L_k \cdot \dot{x}_k(t) + \frac{1}{C_k} \cdot \int_0^t x_k(\tau)d\tau$$

$$-\frac{1}{C_k} \cdot \int_0^t x_{k,k+1}(\tau)d\tau = 0 \qquad (3)$$

$$\frac{-1}{C_k} \cdot \int_0^t x_k(\tau)d\tau + \left(\frac{1}{C_k} + \frac{1}{C_{k,k+1}} + \frac{1}{C_{k+1}}\right) \cdot \int_0^t x_{k,k+1}(\tau)d\tau$$

$$-\frac{1}{C_{k+1}} \cdot \int_0^t x_{k+1}(\tau)d\tau = 0$$

$$\frac{-1}{C_N} \cdot \int_0^t x_{N-1,N}(\tau)d\tau + R_N \cdot x_N(t) + L_N \cdot \dot{x}_N(t)$$

$$+ \frac{1}{C_N} \cdot \int_0^t x_N(\tau)d\tau = 0$$

$U_{-1}(t)$ is the step function: $U_{-1}(t) = 0$ for $t < 0, U_{-1}(t) = 1$ for $t \geq 0$. This set of equations can be solved by use of the Laplace method[6]. The method consists of four steps: transformation into the complex domain $s = \alpha + i\omega$, solution of the complex linear set of equations, fractional decomposition of the solution and inverse transformation into the time domain. We assume that at the time when the driving term $e(t)$ was switched on, i.e. at $t = 0$, there was no stored energy in the system. The Laplace transformation of (3) and the elimination of all transforms of the coupling currents give a new set of N linear equations. Transforms of $x_k(t)$ are denoted here by $\mathcal{X}_k(s)$. The new set of equations is:

$$z_1(s) \cdot \mathcal{X}_1(s) + a_1 \cdot \mathcal{X}_2(s) = \mathcal{E}(s) \cdot s \cdot C_1 = E(s)E(s) \cdot s \cdot C_1 = E(s)$$

$$d_1 \cdot \mathcal{X}_1(s) + z_2(s) \cdot \mathcal{X}_2(s) + a_2 \cdot \mathcal{X}_3(s) = 0$$

$$\vdots$$

$$d_{k-1} \cdot \mathcal{X}_{k-1}(s) + z_k(s) \cdot \mathcal{X}_k(s) + a_k \cdot \mathcal{X}_{k+1}(s) = 0 \qquad (4)$$

$$\vdots$$

$$d_{N-2} \cdot \mathcal{X}_{N-2}(s) + z_{N-1}(s) \cdot \mathcal{X}_{N-1}(s) + a_{N-1} \cdot \mathcal{X}_N(s) = 0$$

$$d_{N-1} \cdot \mathcal{X}_{N-1}(s) + z_N(s) \cdot \mathcal{X}_N(s) = 0$$

$\mathcal{E}(s)$ is the transform of $e(t)$. Coefficients are given by the expressions:

$$a_k = \frac{-1}{1 + \frac{C_{k+1}}{C_k} + \frac{C_{k+1}}{C_{k,k+1}}} \qquad \text{for} \quad k = 1...N-1$$

$$d_k = \frac{-1}{1 + \frac{C_k}{C_{k+1}} + \frac{C_k}{C_{k,k+1}}} \qquad \text{for} \quad k = 1...N-1$$

$$z_k(s) = C_k \cdot L_k \cdot s \cdot s + C_k \cdot R_k \cdot s + b_k \qquad for \quad k = 1...N$$

where:

$$b_1 = 2 - \frac{1}{1 + \frac{C_1}{C_2} + \frac{C_1}{C_{1,2}}} \qquad b_N = 2 - \frac{1}{1 + \frac{C_N}{C_{N-1}} + \frac{C_N}{C_{N-1,N}}}$$

$$b_k = 2 - \frac{1}{1 + \frac{C_k}{C_{k-1}} + \frac{C_k}{C_{k-1,k}}} - \frac{1}{1 + \frac{C_k}{C_{k+1}} + \frac{C_k}{C_{k,k+1}}} \qquad \text{for} \quad k = 2...N-1.$$

Equations (4) may be written in the matrix form:

$$Z(s)X(s) = E(s) \tag{5}$$

$Z(s)$ is a tridiagonal matrix, $X^T(s) = (\mathcal{X}_1(s)...\mathcal{X}_N(s))$ and $E^T(s) = (E(s), 0...0)$. The solution to this equation is the following:

$$\mathcal{X}_k(s) = \frac{\Delta_{k1}(s)}{\Delta(s)} \cdot E(s) \tag{6}$$

for $k = 1 ... N$.

In (6), $\Delta(s)$ and $\Delta_{k1}(s)$ are, respectively, the determinant of $Z(s)$ and the cofactors of the kth row and the first column. All functions $z_k(s)$ are 2nd order polynomials, so $\Delta(s)$ must be a polynomial of order 2N:

$$\Delta(s) = \eta_{2N} \cdot s^{2N} + \eta_{2N-1} \cdot s^{2N-1} + ...\eta_1 \cdot s + \alpha_0$$

and $\Delta_{k1}(s)$ are polynomials of n = 2 (N-k) order:

$$\Delta_{k1}(s) = P_k \cdot (\zeta_{n,k} \cdot s^n + \zeta_{n-1,k} \cdot s^{n-1} + ...\zeta_{1,k} \cdot s + \zeta_0) \tag{8}$$

where:

$$P_1 = 1, \quad P_k = \prod_{j=1}^{j=k-1} a_j \quad \text{for } k = 2...N-1.$$

Two FORTRAN subroutines, have been prepared to find η_j and ζ_{ij} from the replacement circuit elements and to compute precisely the complex solutions s_j to the equation $\Delta(s)=0$. The precise computation of s_j is important when a structure has many weakly coupled cells. For such a structure the dispersion curve is flat and differences betweeen the sequential resonant frequencies are small. Assuming that the source $e(t) = E_0 \cdot \sin(\omega_0 t)$, $\mathcal{X}_k(s)$ may be expanded in a form which makes the inverse transformation easier:

$$\mathcal{X}_k(s) = \sum_{j=1}^{2N} \frac{A_{kj}}{s - s_j} + \frac{A_{k,2N+1}}{s - i\omega_0} + \frac{A_{k,2N+2}}{s + i\omega_0} \tag{9}$$

The coefficients A_{kj} for j = 1 ... 2(N+1) are defined by (6).

Conjugation of solutions $s_j = \alpha_j + i\omega_j = (s_{j+1})^*$ and coefficients $A_{kj} = \gamma_{kj} + i \cdot \chi_{ki} = (A_{k\,j+1})^*$ for $j = 1, 3, 5 \,..,\, 2N + 1$, causes the inverse transformation into the time domain to give the following final results:

$$x_k(t) = 2 \cdot \sum_{j=1,3,5..}^{2N+1} \exp(\alpha_j \cdot t) \cdot [\gamma_{kj} \cdot \cos(\omega_j \cdot t) - \chi_{kj} \sin(\omega_j \cdot t)], \qquad (10)$$

where:

$\alpha_{2N+1} = 0$ and $\omega_{2N+1} = 2 \cdot \pi \cdot f_0$ represent the driving source and $k = 1...N$.

Here we should make two remarks. Firstly, expression (10) describes the response in cell k of the structure for any source frequency f_0 and not only for one of the resonant frequencies f_j. However, the latter are the most interesting. Secondly, the driving term coefficients: $\gamma_{k,2N+1}$ and $\chi_{k,2N+1}$ give the amplitude and phase of the steady state signal $(t \rightarrow \infty)$ in cell k.

3. DISCUSSION

3.1   1 GHz structure, computation and measurement

As already mentioned, the measured response signals in a 1 GHz, 9–cell copper structure with electric coupling $\kappa = 1.85$ and $Q_0 = 25000$ showed no difference in time delay at the beginning of the filling for various resonant modes. Figures 4a, 5a and 6a are response signals measured in cell No.9 after the generator had been switched off. The signals have been measured for three resonant frequencies $f_{\pi/9} = 982.0$ MHz, $f_{5\pi/9} = 992.3$ MHz and $f_\pi = 999.6$ MHz. The modulation we observed here is the same as that of switching on, shifted with offset equal to the constant voltage
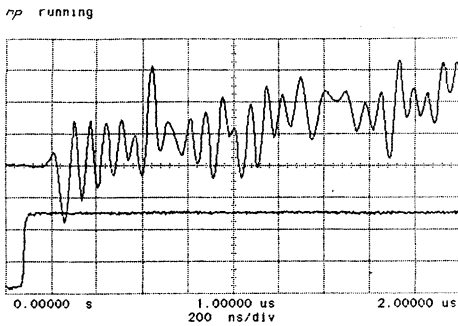
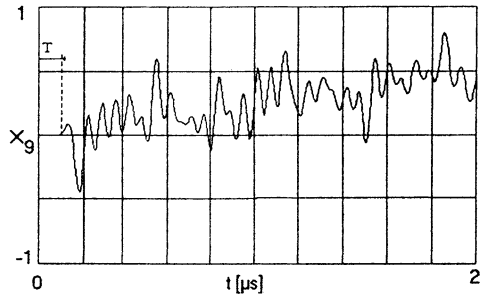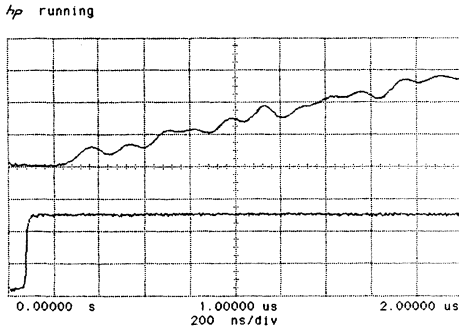a.   b.

FIGURE 4: Measured (a) and computed (b) response of cell No.9 during filling of the cavity. Source $f_0 = f_{\pi/9} = 982.0$ MHz
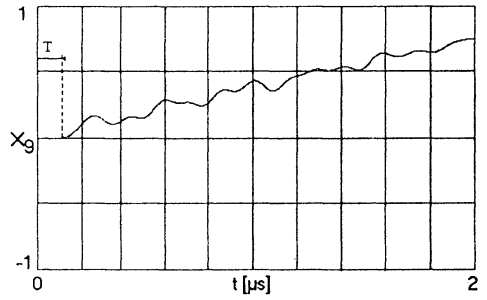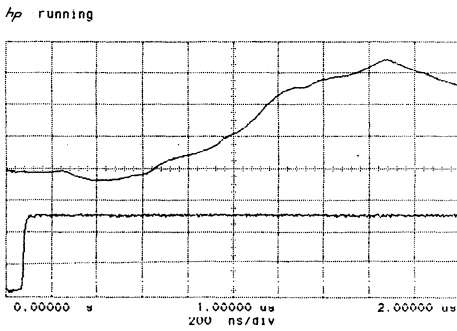
a.
b.

FIGURE 5: Measured (a) and computed (b) response of cell No.9 during filling of the cavity. Source $f_0=f_{5\pi/9}=992.3$ MHz
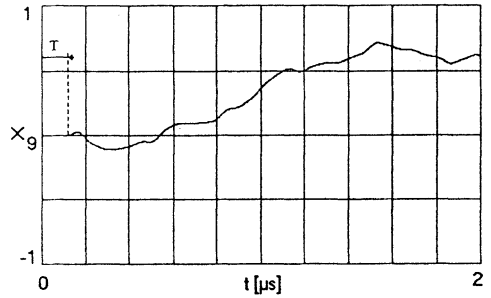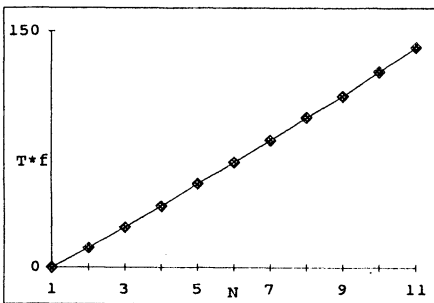
a.
b.

FIGURE 6: Measured (a) and computed (b) response of cell No.9 during filling of the cavity. Source $f_0=f_{\pi}=999.6$ MHz
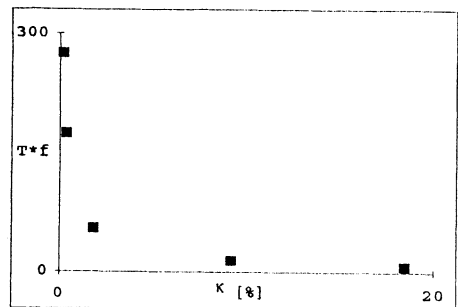
a.
b.

FIGURE 7: a. Signal delay in the last cell vs. N, $\kappa = 1.85\%$
b. Signal delay in the last cell vs. κ, N = 5.

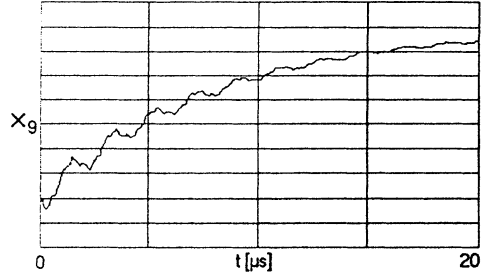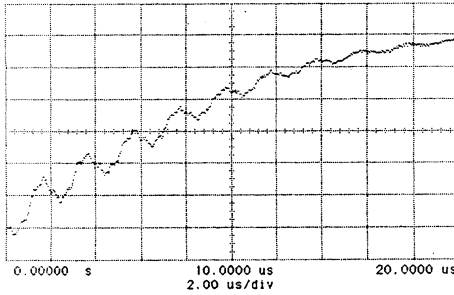a.   b.

FIGURE 8: Measured (a) and computed (b) response in cell No.9 to switching off of the generator. $f_0 = f_\pi = 999.6$ MHz

being the response of the diode to the steady state signal. This way of measurement allows the observation of both increase or decrease of the amplitude without changing of the sign due to the positive or negative diode characteristics. The second curve in each graph shows the envelope of the driving source. Figures 4b, 5b and 6b present computed signals in cell No.9. The driving source was placed, both for measurements and computations, in the first cell. Measured and computed signal delay between this cell and cell No.9 was T = 120ns, independent of the the source frequency. The reason for this is the fast switching on (off) of the source which always excites all passband modes, which decay afterwards, since finite Q makes $\alpha_j < 0$ for $j = 1...N$. The delay was defined as $T = t_N - t_1$ where t_N is the time at which the amplitude in the last cell, N, has the same value as the amplitude in cell No.1 after 10 oscillations, i.e. at $t_1 = 10/f_0$. Further computation showed that the signal delay, T, is proportional to the number of cells N, varies strongly with κ and has rather weak dependency on Q for reasonable wall and external losses. Fig. 7a,b present delay versus N and κ. In both diagrams the delay is normalized and expressed in number of oscillations. Fig. 8a and 8b show measured and computed response in the last cell to switching off of the driving generator for the π–mode over the longer time scale. The similar good agreement of both curves for the whole transient time was also observed for all cells and the other resonant modes. Steady state amplitudes and phases are given, as we noticed before, by coefficients of the driving term in expression (10). Any steady state oscillation of a real multicell cavity requires energy flow along the structure since part of the stored energy lost in the cavity wall must be refilled. The LEC model, which describes properly the transient state of a monoperiodic cavity, shows that energy flow in steady state π–mode is only possible if there is a phase deviation from the ideal lossless case (currents should flow through coupling elements). Fig. 9 presents computed phase deviations $\Delta\phi$ for different Q values in each cell of the 9–cell structure with $\kappa = 1.85$ %. It was assumed for this computation that the source frequency is $f_0 = f_\pi$.
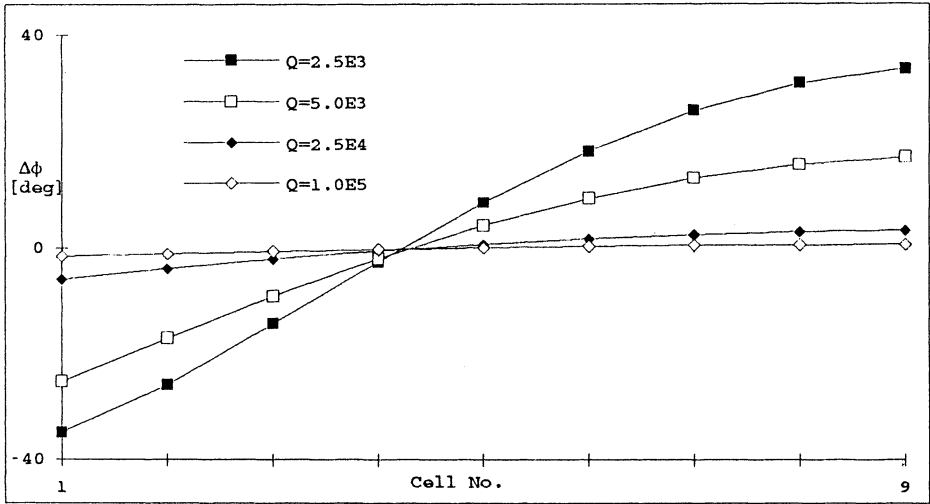
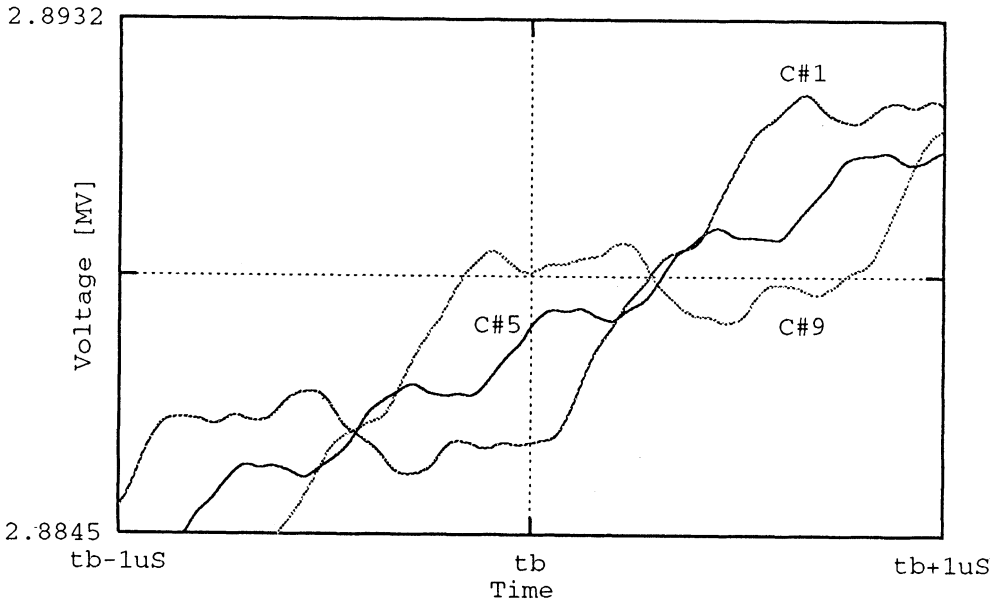FIGURE 9:   Phase deviation from ideal π–mode caused by losses in 9–cell cavity with κ = 1.85 %.

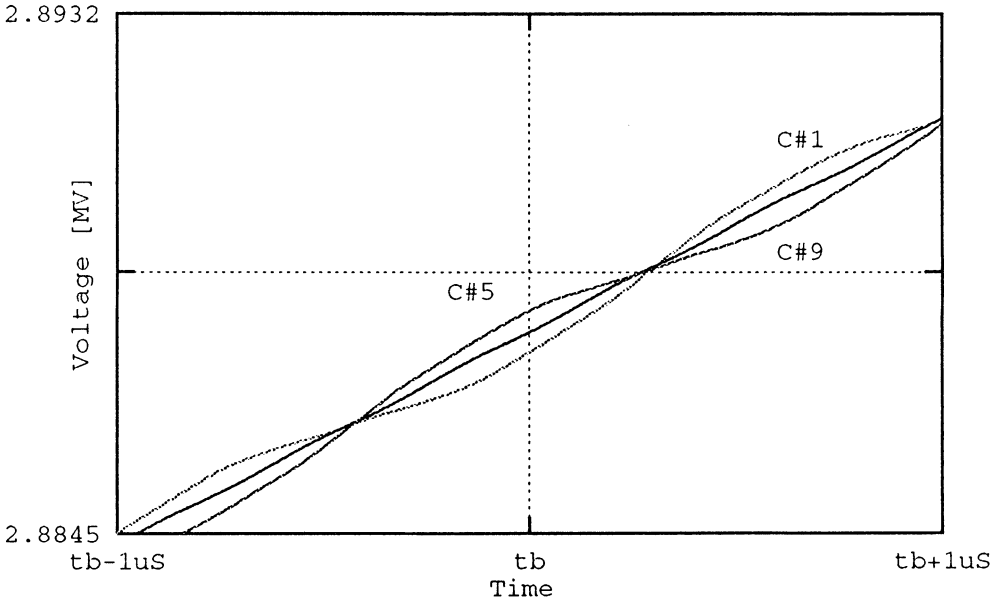FIGURE 10:   Voltage in cells 1,5 and 9 for t in the interval $<tb-1\mu s, tb+1\mu s>$, $to = 0\mu s$

FIGURE 11:   Voltage in cells 1,5 and 9 for t in the interval $<tb-1\mu s, tb+1\mu s>$, $to = 10\mu s$

3.2   TESLA structure

The parameters of the TESLA cavity are as follows: N = 9, Ql = 3.6E6, κ = 1.87%, f_π = 1.3GHz and $\frac{R}{Q}$ = 1030Ω. It is planned that in operation each cavity will be powered with 208kW during a 1.37ms RF pulse. Then the required accelerating voltage of 26MV will be reached at tb=0.57ms. The rest of the RF pulse time is used to accelerate 800 equally spaced bunches, each of 8nC charge. Fig. 10 represents voltages of cell No.1 (input coupler side), No.5 and 9 in the time interval $<tb - 1\mu s, tb + 1\mu s >$, computed for the driving source with infinitesimal rise time of the pulse. The amplitude modulation observed in all cells is due to the eight other modes of the fundamental mode passband which have not completely decayed. The strongest contribution to this modulation is the $\frac{8\pi}{9}$ mode, the amplitude of which in both end cells is 0.05% of the fundamental mode amplitude. It is comparable with the voltage drop of 0.13% in these cells caused by a single bunch. Computations with 2D and 3D codes showed that for a well–tuned cavity all modes except the fundamental one have beam impedances $\frac{R}{Q}$ equal to zero, so no interaction with the accelerated beam and no energy spread between bunches due to this modulation are expected. If the cavity is not well–tuned some energy deviation from the nominal value, caused by the modulation, can occur. On the other hand this residual modulation may be effectively suppressed by increase of the rise time. To simulate pulse of the klystron step function

$U_{-1}(t)$ in the equations (3) was replaced by the function $(1 - exp(-t/to))$. Fig. 11 shows voltages of cell No. 1, 5 and 9 in the same time interval as before, computed for the time to $= 10\mu s$. The suppression of the modulation due to the increase of the pulse rise time is remarkable. We should also note that the mean value of the voltage slope for both rise time values in all cells shows that $1\mu s$ time spacing between the bunches should be enough to refill stored energy in all cells of the cavity.

ACKNOWLEDGEMENTS

REFERENCES

1.   H. Henke, M. Filtz, *Envelope Equations for Transients in Linear Chains of Resonators*, Proc. of the Particle Accelerator Conference (Washington DC, USA, 1993) 901.
2.   D. Nagel, E. Knapp, B. Knapp, *Coupled Resonant Model for Standing Wave Accelerator Tanks*, Rev. of Scient. Instr. **38** Number 11, (1967) 1583.
3.   J. Sekutowicz, Chen Yinghua, Wei Yixiang, *A Different Tuning Method for Accelerating Cavities*, Proc. of the 4th Workshop on RF Superconductivity KEK, Tsukuba (1989) 849.
4.   J. Sekutowicz, S. Kulinski, M. Pachan, *Frequency Dependent Capacitive–Inductive Model for Axially Coupled $\frac{\pi}{2}$ Standing Wave Biperiodic Structure*, IEEE Trans. on Nucl. Sci. Vol. NS–32 (1985) 2824.
5.   G. Geschonke, D. Proch, *Summary of Working Group No.4: Superconducting Linear Collider*, Proc. of ECFA Workshop on e^+e^- Linear Collider LC92, Garmisch Partenkirchen (1992) 407.
6.   P. Pfeiffer, *Linear System Analysis* (McGraw-Hill EAEEE Series)(1961).